# Planning the restoration of membranes in RO desalination using a digital twin

Frits van Rooij*
*Operational Technology Dep., IDE Americas Inc., USA. E-mail: fritsvr@ide-tech.com*

Philip Scarf
*Cardiff Business School, Cardiff University, UK. E-mail: scarfp@cardiff.ac.uk*

Phuc Do
*CRAN - Lorraine University, France. E-mail: phuc.do@univ-lorraine.fr*

*corresponding author

ABSTRACT: This paper describes the development of a decision support system (DSS) for evaluating membrane restoration strategy. The engine of the DSS is a digital twin (DT), a virtual representation of wear (degradation) and restoration of membrane elements in a reverse osmosis (RO) pressure vessel. The basis of the DT is a mathematical model that describes an RO vessel as a novel multi-component system in which the wear-states of individual elements (components) are quantified and elements can be swapped or replaced. This contrasts with the contemporary presentation in the literature of a membrane system as a single system. We estimate the parameters of the model using statistical methods. We describe our approach in the context of a case study on the Carlsbad Desalination Plant in California, which suffers from biofouling due to seasonal algae blooms. Our results show a good fit between the observed and the modelled wear-states. Competing policies are compared based on risk, cost, downtime, and number of stoppages. Projections indicate that a significant cost-saving can be achieved while not compromising the integrity of plant.

*Keywords*: Biofouling, algal bloom, restoration, maintenance, multi-component system, digital twin.

## 1. Introduction

The shortage of freshwater sources around the globe has led to an increased focus on reverse osmosis (RO) desalination to meet clean-water demand for both industrial and domestic use [1-3]. Desalination is now a multi-billion industry. However, membrane fouling significantly impacts the efficiency of RO technology and biofouling is regarded as the most severe and the most difficult to manage [4-6], and algal blooms are the principal, root cause of biofouling in RO membranes [7-10]. In particular, desalination plant on the Pacific coast (California and Chile), the Middle East (the Red Sea and the Persian Gulf coasts) and China report that operations are impacted by algal blooms [1].

Mitigation of biofouling by improving the pre-treatment should be considered [4,8,11-13]. However, this is often limited for economic, environmental, or practical reasons, so that operations and maintenance (O&M) teams often must accept a degree of biofouling. Furthermore, when biofouling is severe, the cleaning of membranes in-situ, so-called cleaning-in-place (CIP), is not sufficient to restore an RO train to an acceptable state. Replacement of the most fouled membrane

elements then becomes unavoidable [2]. Membrane maintenance can become costly when the number of elements replaced surpasses that initially projected in the plant-design phase.

Biofouling is estimated to cost the desalination industry worldwide an estimated $15 billion annually [3]. Despite the potential severity of biofouling and the costly consequences, little attention is given so far in the literature on the management of membrane restoration. Mitra et al. [4] reported a decision, after three years of operation, to replace 25% of membrane elements in a plant in one go. They discussed the performance effect but not the cost-efficiency of this intervention. Vrouwenvelder et al. [5] and Bartman et al. [6] developed a simulation tool for monitoring biofouling in spiral-wound membranes. This tool notionally monitors the first element in a vessel, so that a complete picture of the states of all elements in the vessel is missing. Koutsakos and Moxey [2] describe a protocol for membrane maintenance. The first step is CIP, and the second step is replacement or swapping of elements if CIP is not sufficiently effective. While their system records the position of every element in an RO train, it quantifies neither the states of elements nor the long-run costs of interventions.

In our paper, we propose a new approach that quantifies the wear-states (degradation) of each membrane element throughout the life of a train. This allows the effect of swapping elements or inserting a new element at a particular position to be predicted. Our model is the basis for a digital twin of an RO train that is used to evaluate different maintenance strategies, in cost and performance terms. We apply our approach at the Carlsbad RO Desalination Plant in California. This plant is the biggest and most sophisticated in the Western Hemisphere and suffers significant biofouling due to seasonal algae blooms. Our solution has the potential to reduce the costs of O&M companies by optimizing membrane replacement management and CIP scheduling. We demonstrate that the solution does not require a large investment and that implementation is practicable. The approach eliminates ad hoc decision-making about membrane replacement and, in our opinion, sets a new gold-standard for membrane maintenance management.

The crux of our approach, and the model that underlies it, is the modeling and quantification of rate-state interactions in the degradation of multi-element systems [7, 8]. Rate-state interaction parameters are estimated using real data on vessel performance. A further novel aspect of the model is that the wear-states of the individual elements are themselves hidden (unobservable). Nonetheless, we are able to estimate them, and thereby quantify the effect (on performance) of element replacements and swaps. Although we focus on biofouling, our model is not limited to this, and potentially can be used in cases of mineral scaling.

The structure of the paper is as follows. Section 2 describes the context and details of the system and biofouling. Section 3 gives the mathematical detail of the model. Estimation of model parameters (Section 4), the development of the digital twin and the decision support system (Section 5), and analysis of the restoration policies (Section 6) are then described. We conclude with a discussion of the effectiveness of our approach, its limitations and scope for further development.

## 2. System description and analysis

There are more than 2000 pressure vessels in the Carlsbad Desalination Plant. Of these 1932 vessels belong to the 1st Pass RO system and of these 1792 are filled with membrane elements. The rest are spare for future expansion of production. The vessels are divided into 14 stacks, and each

stack is referred to as an RO train. Thus, there are 128 vessels in parallel in each train. Each vessel is loaded with eight identical (when new) elements. Vessels hold a single type of membrane element, specifically the FilmTec™ SW30HRLE-400 (active area of 37 $m^2$; spacer thickness 28 mil (0.7mm); permeate flow rate 28 $m^3$/day; salt rejection of 99.8%).

Clarified seawater enters the feed and the concentrated rejected brine is discharged at the tail of the vessel. The front permeate goes directly to the post-treatment for re-mineralization. The rear goes first to a brackish water RO system for further desalination. The membrane elements are spirally wounded with a fine feed water carrier to allow the seawater to be pushed across the membrane surface of all the elements from the feed of the lead element to the tail of the last element. Resistance in the feed water carrier results in a small hydraulic pressure-drop across each element. This is the pressure differential (PD) of a new element.

Each train is operated and monitored independently of every other, and demand for permeate (drinking water) is typically met when 13 of the 14 trains are operating. More precisely, the mean peak demand for water from the plant is 204 $Km^3$/day and recommended allowable maximum supply per train is 631 $m^3$/hour.

### *2.1. Deterioration of the membranes due to biofouling*

Degradation of the membranes due to fouling manifests as a decrease in permeate flow, an increase in salt passage and an increase in pressure differential (PD) [9, 10, 11]. Biofouling in particular increases the PD due to the build-up of the biofilm between the membrane surface and the feed water carrier [10-13, 21]. Therefore, PD provides a measure of the level of wear of an RO train.

However, permeate flow, salt passage and PD vary without deterioration of the membranes due to changes in feedwater temperature, salinity and flows. To enable monitoring of membrane deterioration, the effects of feedwater temperature, salinity and flows must be filtered out. The process of standardizing RO performance data is defined in the industry as *normalization*. The American Society for Testing Materials (ASTM) defines the standard practice for standardizing RO performance data in ASTM Methods 4516, but there is no specification for PD normalization in this standard [12]. We use a normalization equation that was specified by the membrane manufacturer. RO real-time performance data is monitored continuously and recorded in intervals of 60 seconds. The normalized pressure differential (NPD) is calculated from the hourly means of the recorded data. Then, to reduce noise from e.g., stoppages, at 00:00 hours every day the mean NPD is calculated over the previous 24 hours. This daily mean NPD provides a measure of the level of deterioration of the vessels in an RO train (Fig. 1).

The effect of bio-fouling is continuous and long-lasting and regarded as the most severe and the most difficult to manage. Initially, organic macro-molecules, mainly anionic biopolymers, settle on the surface of a clean membrane and form a conditioning film. This film increases the capacity of the surface to absorb and concentrate nutrients from the RO feed water. Bacterial species that produce large amounts of extracellular polymeric substances then colonize the surface, forming a slime layer, known as a “biofilm”. This biofilm harvests nutrients and protects bacteria. Depending on the supply of nutrients, the biofilm can grow in a matter of days or even hours. When this biofilm starts affecting the RO system, operators speak of biofouling [9, 10, 11].

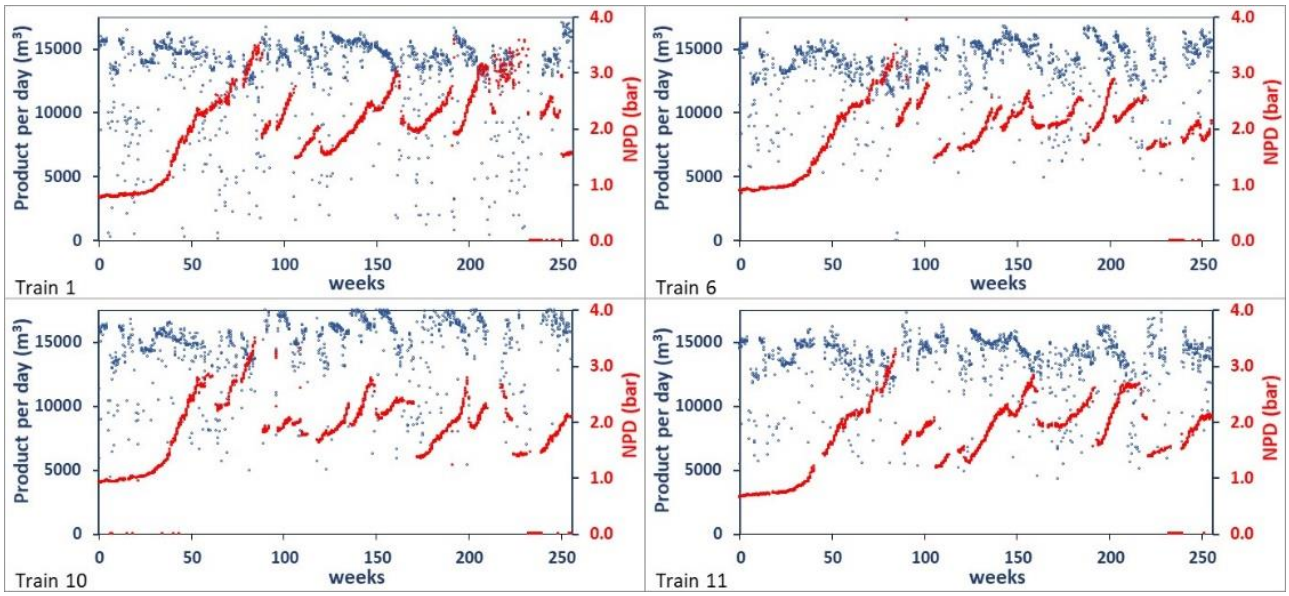


**Fig. 1.** Product flow-rate and normalized pressure differential (NPD) for a selection of the 14 trains at Carlsbad from the start of operation of the plant up to September 2020.

Algal blooms accelerate biofouling in RO membranes. Specifically at the Carlsbad plant, Table 1 summaries the condition of the RO feed water. The direct cause of the accelerated deterioration is not the algae cells themselves but algae-derived organic matter (AOM), particularly transparent exopolymer particles (TEP). Dead algae cells disintegrate and release AOM, which adheres to clean membranes and even more so to AOM-fouled membranes, thus reinforcing the biofouling. This is extrinsic wear originated from shared physical or environmental stresses [13]. Extrinsic wear is captured in the model. Further, high absorption of TEP can be observed as a slimy substance, sticking to every surface. Dinoflagellates, a group of phytoplankton responsible for algal blooms, generate large quantities of TEP once nutrients have been exhausted [14]. Therefore, the degradation due to bio-fouling continues beyond the period of an algal bloom. Also, the state of an element influences its wear-rate because algal contamination adheres more to worn elements, so providing more nutrients, therefore stimulating bacteria cultivation, thus reinforcing the biofouling [1, 15].

**Table 1**
Average RO feed source water condition during algae bloom and non-algae bloom conditions (2017-2020) (ND = non detect). When SDI > 5 and/or Turbidity > 0.35 NTU, feed water supply is interrupted.

| | SDI | Turbidity (NTU) | 2-5 µm particle (counts/ml) | ORP (mV) | DOC (ppm) | TOC (ppm) |
|---|---|---|---|---|---|---|
| non-algae bloom | 3.08 | 0.07 | 41.59 | 222.51 | ND | 0.71 |
| algae bloom | 4.62 | 0.13 | 157.47 | 232.12 | 1.88 | 2.21 |

Thus, degradation of the membrane in a vessel due to biofouling is not homogeneous, with the lead side tending to degrade faster than the tail side due to the attachment, growth and dispersal of bacteria [16]. Further, the pressure vessel contains distinct, replaceable elements or components. Therefore, from the perspective of maintenance modeling theory, an RO vessel can be considered a multi-component system with non-identical components [17], with stochastic dependence between

components [18] in which the rate of wear of one component (membrane element) depends on both its position and the state of the others. This is so-called rate-state wear-dependence [7, 8, 19]. This rate-state dependence is captured in our model in a way that is different to wear models for multi-component systems that have been considered to date. For a recent review of such models, see de Jonge and Scarf [20]. The degradation processes of membranes are mathematically developed and presented in Section 3.

### *2.2. Restoration of membranes*

Regarding now the management of wear, a vessel can be partially restored by various methods:

- Cleaning is restoration in which biomass is partially removed from all elements. For the trains in Fig. 1, for example, two cleaning methods were used. The first (C1) is a standard cleaning method in which low pH cleaning follows high pH cleaning (Table 2). The second (C2) soaks the elements with sodium bisulphate (1% solution, 0.7 $m^3$/h per vessel for 24 hr) and then proceeds as C1.

**Table 2**
Procedure for high and low pH cleaning-in-place (C1)

| | pH | Chemical | Stage 1<br>low flow per vessel | Stage 2<br>high flow per vessel | Stage 3<br>Soaking | Stage 4<br>high flow per vessel |
|---|---|---|---|---|---|---|
| High pH | 12 | NaOH | 4 $m^3$/h (15 min) | 7 $m^3$/h (60-90 min) | 60 min | 7 $m^3$/h (60 min) |
| Low pH | 2 | HCl | 4 $m^3$/h (15 min) | 7 $m^3$/h (30-45 min) | 30 min | 7 $m^3$/h (60 min) |

- Cascading is a combination of partial replacement and component reallocation [21] that aims to replace elements with the most accumulated biomass. The membrane element in the leading socket (S1) in each vessel is, typically, replaced by the element in the second socket (S2), that in S2 by that in S3, and so on, and a new element is placed in S8. In general, $r$ elements can be replaced, and 8-$r$ cascaded.
- Swapping is another component-reallocation intervention that partially restores a vessel. Elements in leading sockets are systematically swapped with elements in trailing sockets, and no new elements are used [22].

The restoration history up to week 260 for the trains shown in Fig. 1 are given in Table 3.

**Table 3**
Membrane restoration history since start operation for trains 1, 6, 10, and 11. C1: clean-in-place method 1. C1: clean-in-place method 2; MR: partial membrane replacement.

| Train 1 | | Train 6 | | Train 10 | | Train 11 | |
|---|---|---|---|---|---|---|---|
| week | action | week | action | week | action | week | action |
| 104 | MR | 102 | MR | 84 | MR | 85 | MR |
| 119 | C1 | 141 | C1 | 109 | C1 | 104 | MR |
| 166 | C2 | 158 | C2 | 136 | C1 | 121 | C1 |
| 191 | MR | 185 | MR | 150 | C2 | 161 | C2 |
| 210 | C2 | 202 | C2 | 171 | MR | 192 | MR |
| 251 | MR | 219 | MR | 200 | C2 | 218 | C2 |
| | | 248 | C1 | 223 | MR | 220 | MR |
| | | | | 255 | C2 | | |

With cascading and swapping, elements are always inserted from the lead (seawater) to the tail (brine) side of the vessel to prevent displacement or damage to the o-rings of the element interconnectors. Such damage would result in saltwater leakage into the permeate water tube. Thus, when an element in S*n* is removed, elements in S1 to S*n-1* must be removed. From the point of view of maintenance theory, this is structural dependence [23, 24], while the positional dependence, discussed above, is structural-performance dependence [25]. Furthermore, cascading and swapping are membrane interventions with a fixed set-up cost (vessel opening) so that the multi-component system (vessel) exhibits economic dependence [26].

Full restoration, in theory, is the replacement of all $n$ elements in a vessel by new elements. However, this is prohibitively expensive, because it cannot be limited to a single vessel as the states of all vessels in a train must be balanced. When there are vessels in parallel with different states, a vessel with less wear has higher flux than other more worn vessels and so degrades faster. This accelerated wear then brings the vessel to the same state as the other vessels over time. This is also the case when operating trains in parallel in a pressure centre configuration (multiple trains sharing the same pump) as is the case at the Carlsbad plant. Therefore, trains are managed collectively whereby trains are operated and maintained to keep both the flux and the state of the trains balanced. Nonetheless, some differentiation between trains is unavoidable. This is because trains must be taken offline for restoration or due to the reduction of demand. Note: when a train is offline for several days, it is flushed with permeate water, which has low salinity (LS). Since the nutrient-rich seawater is displaced with nutrient-poor LS water, biofouling is slowed down. LS flushing does not remove the matured biofilm, therefore this slowdown is only temporary. For this reason, we ignore the effect of LS flushing in our model. Thus, in the model, we assume that the states of vessels in the same train are identical, but trains are not. Therefore, the model we build considers a single, idealized vessel in a train.

## 3. Mathematical modeling

Conceptually, a vessel has $n$ sockets in series and an element is placed in each socket. It is convenient to define sockets and elements (components) in this way because the sockets are fixed while elements can be replaced or swapped. This conceptual notion of sockets and elements is standard terminology in maintenance modeling that was first used by Ascher and Feingold [27].

The wear-state of the element in socket $i$ at time $t$ is $X_{i,t}$, and the (unobserved) pressure-differential across socket $i$ is $P_{i,t}$, $i = 1,...,n$. The pressure-differential across the vessel (and hence all parallel vessels in the train), which is observed, is given by

$$P_t = \sum_{i=1}^{n} P_{i,t} \,. \tag{1}$$

When an element is new, we suppose that its state is $X_0 = 1$, and when a vessel is new (all elements are new) its pressure-differential is $P_0$.

Note, when we discuss this conceptual model, we will refer to *pressure differential* (PD), but when we discuss the reality we shall refer to the *normalized pressure differential* (NPD), which is the observed pressure differential after the pre-processing discussed above in Section 2.1.

*3.1. Modeling the pressure distribution*

The hydraulics of saline flow in an RO vessel (Fig. 2) implies that the pressure-differential $P_{i,t}$ across socket $i$ at time $t$ depends both on the state of the element in socket $i$ and the position of the socket. Therefore, it is reasonable to assume that

$$P_{i,t} = \omega_i P_0 X_{i,t},\ i = 1,...,n, \tag{2}$$

with $\omega_i$ $(i = 1,...,n)$ a set of known (dimensionless) constants such that $\sum_{i=1}^{n} \omega_i = 1$. We call these constants the pressure-position distribution. They represent the pressure variation due to position.

The variation $\omega_i$ arises broadly because the salinity of the feed at each element increases along the vessel. In simplified terms, a vessel has a feed (saline) side and a permeate (drinking water) side. A vessel is a sequence of elements in series. Seawater is pumped into a vessel under high pressure and flows first into element 1 then into element 2 and so on. Water passes through a membrane element provided there is a positive net driving pressure, that is, provided the pressure on the feed-side ($P_{feed}$ in Fig. 2) is higher than the osmotic pressure ($\Pi$ in Fig. 2). The net driving pressure is $P_{\text{feed}} - P_1 / 2 - \Pi_1 - P_{\text{permeate}}$ at element 1 and $P_{\text{feed}} - \sum_{j=1}^{i-1} P_j - P_i / 2 - \Pi_i - P_{\text{permeate}}$ at element $i$ $(i = 2,...,n)$, where $\Pi_i$ is the osmotic pressure of the feed/brine side minus the osmotic pressure of the permeate side of the element.

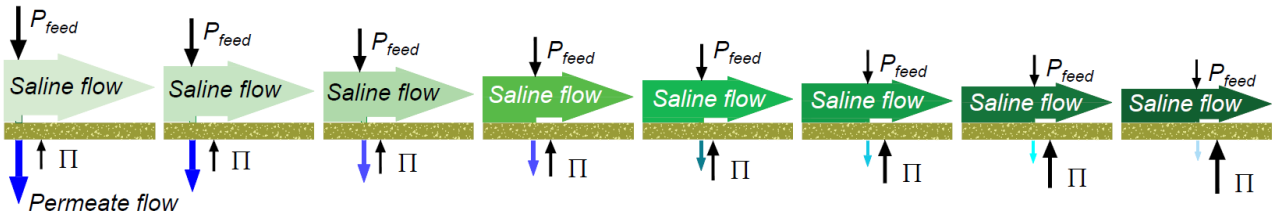


**Fig. 2.** Hydraulic representation of an RO vessel with eight membrane elements

$P_{\text{feed}}$ decreases from one socket to the next. This decrease is the pressure-differential across a socket and is a function of the state of the membrane element in that socket. The osmotic pressure is a function of the relative salinities of the feed and the permeate, noting that the permeate is not perfectly desaline. Thus, the osmotic pressure is that difference in pressure between the feed and permeate side of a perfect membrane such that water just starts to pass to the permeate side and salt is retained on the feed side. The higher the salinity, the higher is the osmotic pressure. As a membrane wears, that is, as it becomes biofouled, its feed-brine pressure-differential increases. Now, assuming there is permeate flow, that is, the feed pressure is sufficiently high, as water flows on the feed-side from one element to the next, the salinity of the feed-side increases from one element to the next so that the osmotic pressure increases from one element to the next, and the permeate flow-rate through each element correspondingly decreases. The permeate flow rate of an element depends on the difference between the feed-side pressure and the osmotic pressure.

Now, consider a vessel with a set of new elements. We define the saline flow per element as $Q_i$ and the permeate flow per element as $\overline{Q}_i$. Recovery is defined as

$$R_i = \overline{Q}_i / Q_i .$$

We assume that the recovery reduces proportionally with the increase of salinity of the feed. Furthermore, the salt rejection rate is 99%. Therefore, the salinity of the feed for socket $i$ relative to

socket $i-1$ increases by the factor $sR_{i-1}$ ($s=0.998$). So, we get $R_i = R_{i-1}/\{1+sR_{i-1}\}$ and recursively we obtain the following:

$$R_i = R_1/\{1+(i-1)sR_1\},\ i=2,...,n. \tag{3}$$

The system recovery is given by $R=\sum_{i=1}^{n}\bar{Q}_i/Q_1$, and since $Q_i = Q_{i-1}(1-R_{i-1})$, we can derive the following:

$$R = R_1 + \sum_{i=2}^{n}\left\{\frac{R_1}{1+(i-1)sR_1}\prod_{j=2}^{i}\frac{1-\left(1-(j-2)s\right)R_1}{1+(j-2)sR_1}\right\}. \tag{4}$$

Because $R$ is known (it is continuously monitored at train level), $R_1$ can be calculated numerically using Eq. (4), and the recoveries for each trailing element can then be obtained from Eq. (3). In this way, we obtain

$$\omega_i = R_i/\sum_{i=1}^{n}R_i,\ i=1,...,n,\ \sum_{i=1}^{n}\omega_i = 1.$$

These constants represent the variation of PD across the sockets in an as-new vessel, and correspond to the Darcy-Weisbach head-loss model that describes the relationship between flow and pressure loss [28]: if the flow reduces, the pressure loss reduces. The constants $\omega_i$ do not depend on the states of the elements. This is a reasonable assumption for a typical vessel under normal operation, although it would not apply under unusual operating conditions, which themselves would jeopardize the integrity of a vessel.

### *3.2. Modeling wear increments*

To model the evolution of the wear-state of the element in socket *i* over time, we discretize time for convenience and use the day as the unit of time. We denote the wear-increment in the element in socket $i$ from day $t-1$ to day $t$ by

$$\Delta X_{i,t} = X_{i,t} - X_{i,t-1}. \tag{5}$$

We suppose this wear-increment is given by

$$\Delta X_{i,t} = \kappa_t \alpha^{i-1}\{\sum_{j=i+1}^{n}X_{j,t-1}/(n-i)\}^{R\gamma}, \tag{6}$$

for $i=1,...,n-1$, and

$$\Delta X_{n,t} = \kappa_t \alpha^{n-1}. \tag{7}$$

Here,

- $\kappa_t$ is the extrinsic (common-cause) wear effect due to the feed water quality on day *t*. Notice that when all elements in the vessel are new (either when the plant is new or hypothetically when all the elements in the vessel are replaced), the wear-increment in the element in socket 1 (S1) is precisely $\kappa_t$ because the other terms are equal to 1.
- $\alpha \in (0,1)$ quantifies the variation in biofouling along a vessel due to preferential attachment of bacteria, and hence the growth of biomass, to leading elements, as discussed in Section 2. This exponential decay is a specific way to model the biofouling-position effect with a single unknown parameter.

- $\{\sum_{j=i+1}^{n} X_{j,t-1} / (n-i)\}^{R\gamma}$ models the wear in an element that accrues because the trailing elements (elements further along the vessel) are worn. This wear interaction is the multi-component rate-state effect [19,20, 28]. The parameter $\gamma$ is the strength of this effect. A vessel generally works harder when its recovery is higher, so that *R* influences this effect in the same way. When the elements in trailing sockets are all new, the term is null. This is justified because the effect of varying recovery is negligible when the vessel is as-new.

When a train is offline, it is flushed daily with seawater (to prevent hydrating the elements). In this case, there is neither rate-state dependent wear nor a recovery effect because the recovery is zero. Thus, the term $\{\sum_{j=i+1}^{n} X_{j,t-1} / (n-i)\}^{R\gamma}$ is unity when the train is offline and the wear-increment is limited to $\Delta X_{i,t} = \kappa_t \alpha^{i-1}$.

### *3.3. Modeling restoration*

When the element in socket $i$ is replaced by a new element at time $t$, we suppose that $X_{i,t^+} = 1$, where $t^+$ denotes the time immediately following the restoration. During any restoration (which typically takes one to two weeks to complete for a train), the vessel is drained, and element states are otherwise unchanged.

When the element in socket $i$ is swapped with the element in socket $j$ at time $t$, then immediately following restoration we have

$$X_{i,t^+} = X_{j,t^-}, \quad X_{j,t^+} = X_{i,t^-}, \tag{8}$$

where $t^-$ denotes the time operation immediately prior to the restoration. In this way, the model captures the state of an element in its socket.

Cleaning can be modelled in a number of ways. We suppose that the cleaning effect is proportional to the wear so that an element in a poorer state is cleaned to a greater absolute extent. Thus, if a vessel is cleaned at time $t$, then the state of the cleaned element in socket $i$ is given by $X_{i,t^+} = (1-\delta)(X_{i,t^-} - 1) + 1 = (1-\delta) X_{i,t^-} + \delta$, and the PD across the vessel (overall) immediately following cleaning is

$$P_{t^+} = (1-\delta) P_{t^-} + \delta P_0 \tag{9}$$

Thus, the cleaning effect is proportional to the excess PD above $P_0$. Here $\delta$ is the cleaning effect parameter. If $\delta = 0$, $P_{t^+} = P_{t^-}$, so cleaning has no effect. If $\delta = 1$, $P_{t^+} = P_0$, so cleaning is as good as a replacement of all elements in the vessel (like new). An absolute cleaning effect would be unnatural because potentially this could imply $P_{t^+} < P_0$.

## 4. Estimation of parameters

We first estimate the biofouling-wear distribution parameter $\alpha$ (see Eq. 6). Once $\alpha$ is specified, we use the particle filter method [29] to estimate $\gamma$ and $\beta$ using a restricted set of values for $\kappa_t$. Then we calculate daily values of $\kappa_t$ for use in predicting future NPD.

The parameter $\alpha$ is estimated by comparing the modelled wear distribution across individual elements with the measured distribution of biomass obtained at vessel inspections, when a vessel is opened and individual elements are weighed. This method is as follows. We fix $\gamma = 1$ (the effect of $\gamma$ on the outcome of $\alpha$ is small so we neglect it). Eqs. (1, 2, 5-7) imply that

$$\kappa_t = \frac{P_t - P_{t-1}}{P_0 \sum_{i=1}^{n} \alpha^{i-1} f\left(x,i\right)^{R\gamma} \omega_i}, \tag{10}$$

where,

$$f\left(x,i\right) = \begin{cases} \dfrac{\sum_{j=i+1}^{n} X_{j,t-1}}{n-i} & i < n, \\ 1 & \text{else.} \end{cases}$$

Then, $\kappa_t$ can be calculated recursively as follows. On day $t = 1$, $X_{i,0} = 1$ (all elements are new), $P_1 - P_0$ is observed (this is the NPD increment), $R$ is known, the constants $\omega_i$ are known, and $\alpha$ is specified (and $\gamma = 1$). Therefore, $\kappa_1$ can be calculated using Eq. (10) and $X_{i,1}$ $(i = 1,...,n)$ can be calculated using Eqs. (6, 7). Then, in turn, $\kappa_2$ can be calculated using $P_2 - P_1$ (observed) and the known $X_{i,1}$ $(i = 1,...,n)$, and so on. When elements are swapped, Eq. (8) is used to update the wear-states. Then, on day $\tau$ when elements in a vessel are weighed, we know the weights $w_i$ and the states $X_{i,\tau}$ of each element (Fig. 3), and the deviation

$$\sum_{i=1}^{n} \left( \frac{X_{i,\tau}}{\bar{X}_\tau} - \frac{w_i}{\bar{w}} \right)^2,$$

can be calculated. The procedure is repeated for different values of $\alpha$ and our estimate is the value of $\alpha$ that minimizes this deviation.

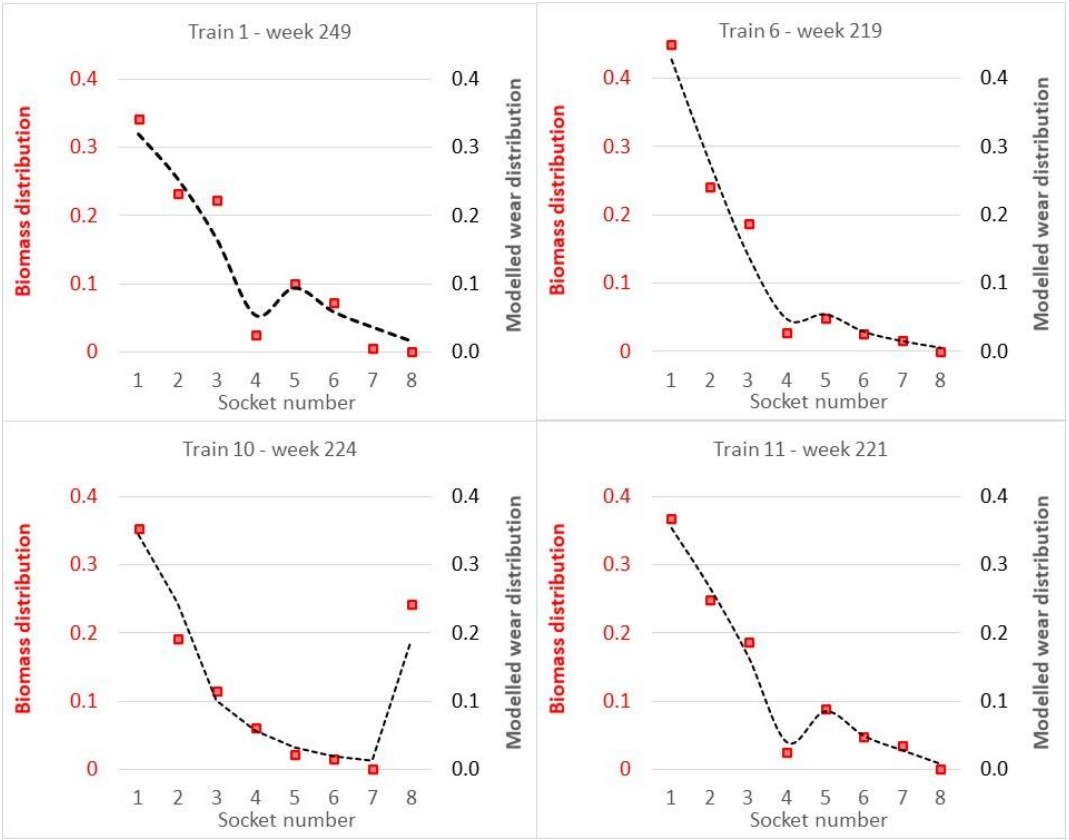


**Fig. 3.** Relative element weights (▪) and relative modelled wear-states (---) for a selection of trains (train number and time of weighing indicated with $\alpha$ at best value for the specific train).

Next, the other parameters are estimated using the particle filter [40] as follows. We have specified a function (Eqs. 2-6) that seeks to model the data (observed NPD). Given the data, some parameter values are more probable than others, and this defines a probability distribution over the parameter space (the set of all possible values of the parameters). Particle filtering uses sequential simulation to approximate this distribution. Then, this distribution can then be used to determine a best estimate (e.g. the mean value of the parameter vector). Further details of the PF algorithm we use are given in Do et al. [41].

We run the PF for each train separately and up to day 500 because there was no element swapping or replacement up to this time. To simplify the problem, we now assume a fixed value $\kappa_1$ up to day 213 (the known start of the first algal bloom) and a different fixed $\kappa_2$ thereafter. To account for the decay in NPD increments after the finish of an algae bloom (due to nutrients stored in the biofilm during an algal bloom [30]), we suppose $\kappa_t$ decays: $\kappa_t = (\kappa_2 - \kappa_1)e^{-\beta\tau}$, where $\tau$ the days since the finish of the algae bloom. This way the estimates of $\gamma$, $\beta$, $\kappa_1$ and $\kappa_2$ for each train (Table 4) are obtained. We do not estimate $\alpha$ using the PF because we wish to use information about $\alpha$ that is available in the measured biomass distribution at the time of the inspection.

**Table 4**
Estimates of parameters.

| **Train** | $R^2$ | *RMSE* | α | $\gamma$ | $\beta$ | $\kappa_1$ | $\kappa_2$ |
|---|---|---|---|---|---|---|---|
| 1 | 0.992 | 0.06 | 0.65 | 0.74 | 0.026 | 0.0014 | 0.025 |
| 2 | 0.964 | 0.10 | 0.65 | 0.73 | 0.026 | 0.0028 | 0.025 |
| 3 | 0.975 | 0.10 | 0.64 | 0.66 | 0.031 | 0.0011 | 0.029 |
| 4 | 0.980 | 0.09 | 0.62 | 0.86 | 0.023 | 0.0017 | 0.024 |
| 5 | 0.984 | 0.08 | 0.47 | 0.80 | 0.023 | 0.0025 | 0.036 |
| 6 | 0.988 | 0.06 | 0.55 | 0.72 | 0.017 | 0.0016 | 0.033 |
| 7 | 0.983 | 0.07 | 0.53 | 0.73 | 0.020 | 0.0010 | 0.032 |
| 8 | 0.983 | 0.09 | 0.66 | 0.92 | 0.023 | 0.0018 | 0.026 |
| 9 | 0.975 | 0.07 | 0.60 | 0.90 | 0.026 | 0.0019 | 0.029 |
| 10 | 0.979 | 0.09 | 0.55 | 0.82 | 0.028 | 0.0021 | 0.031 |
| 11 | 0.990 | 0.06 | 0.60 | 0.86 | 0.014 | 0.0023 | 0.038 |
| 12 | 0.973 | 0.09 | 0.70 | 0.55 | 0.021 | 0.0015 | 0.023 |
| 13 | 0.979 | 0.08 | 0.61 | 0.70 | 0.020 | 0.0011 | 0.022 |
| 14 | 0.969 | 0.07 | 0.74 | 0.54 | 0.034 | 0.0010 | 0.027 |
| mean | 0.980 | 0.08 | 0.60 | 0.75 | 0.023 | 0.0017 | 0.029 |
| min | 0.969 | 0.06 | 0.47 | 0.54 | 0.014 | 0.0010 | 0.022 |
| max | 0.990 | 0.09 | 0.74 | 0.92 | 0.034 | 0.0025 | 0.038 |
| Std | 0.006 | 0.010 | 0.078 | 0.126 | 0.005 | 0.0005 | 0.0047 |

Before using the PF, to improve its accuracy, we first smoothed NPD using the Savitzky-Golay polynomial filter [42] with a polynomial degree of 4 and a moving window of 150 to remove various partial spikes in NPD. These spikes arise when a train is taken offline for a brief period and likely related to low salinity flushing at this time.

Next, to find a set of values of $\kappa$ for projecting the model, we use Eq. (10) to re-calculate $\kappa_t$ daily for each train and smooth these using a moving average. To ensure the results are robust to the smoothing, we use three different smoothing windows, 1 before, 4 after (-1,4), (-2,8), and (-4, 16), corresponding to windows of width 5, 10 and 20 days, respectively. Then, we use the smoothed values to provide bootstrap samples [43] for projection. We assume years are statistically identical so that,

with five years of observed data in total, we obtain five values of $\kappa$ for each day and for each train. Estimates for trains are then pooled, yielding a bootstrap sample of size 70 (5x14) for each day of the year and therefore a 70x365 bootstrap sample matrix. February 29th is ignored.

The cleaning effect $\delta$ was calculated using Eq. (9) for each cleaning operation. Note, the effects of cleaning can have a lag of a few days after a train returns to normal operation, so $P_{t^+}$ must be carefully specified. In total 64 CIP restorations were performed up to September 2020, of which 33 were C1 and 31 were C2. C1 gave on average a reduction of NPD of 14%, however, in one-fifth of the cases it was less than 10%. C2 gave on average a reduction of NPD of 26%. Only in 4% of the cases was the reduction less than the average reduction by C1. The mean $\delta$ for C1 was 0.24 with a standard deviation ($\sigma$) of 0.13. The mean $\delta$ for C2 was 0.38 with a standard deviation of 0.1 (Fig. 4).

Broadly, trains exhibit the same patterns of development NPD (Fig. 1). However, the periods of operation of trains differed and so they are not exposed equally to extrinsic feedwater conditions. Further, subsequent to day 500, trains were subject to different restorations.

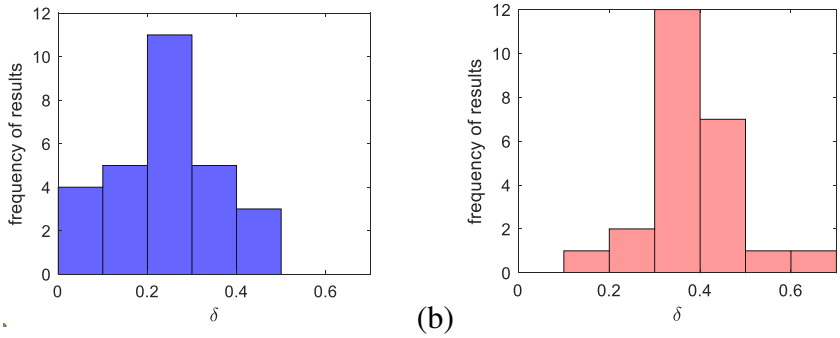


(a) (b)

**Fig. 4.** Histograms of the observed effects for cleaning-in-place for cleaning modes C1 (a) and C2 (b).

## 5. Digital twin of a RO train

A digital twin (DT) was first conceptualized as a finite-element model of an aircraft structure [44], but is now understood as any virtual representation of an engineered object on a computer for the purpose of product or process planning [45]. A DT does not need to represent all characteristics of the physical counterpart but can be limited to the specifics being investigated, using only relevant data and models [46]. The DT bears some similarity to accelerated life testing [47], because a DT can show degradation and failure behaviours without having to wait for the real system to degrade and fail. Equally, interventions, that may slow degradation, prevent failure, restore functionality, and thereby reduce risk and increase performance, can be investigated quickly. Such interventions may extend over the entire product life cycle.

We built a DT of an RO vessel using the mathematical model of degradation described above. The DT is part of a decision support system (DSS). The DSS is a tool, developed in MATLAB, with visualization for planning restoration (Fig. 5). The DSS has three modules: a data analysis module, a planning module, and the DT. The data analysis module allows the user to import real data and maintenance history, estimate parameters, and tune parameters manually. At the visualization (Fig. 5), a simulated trajectory can be compared with a real trajectory. The planning module allows for different restoration policies to be studied. It uses the DT to simulate NPD and cost trajectories for a

specific policy. The DSS displays the modelled NPD (red pen, Fig. 5), calculated using the DT which runs in the background, the observed NPD (black pen), and the NPD implied by the modelled wear of each element in each socket (other coloured pens). The output of the DT shows a good fit between the observed and the modelled states. Then, the user can select a restoration policy and the DT simulates an ensemble forecast over the period of projection (grey ribbon).

This simulation of projected NPD is as follows. First, the current modelled wear of the element in each socket, $X_i$, $(i = 1,...,n)$, is determined. Then, $\kappa$ (feed quality) for each day of the projection is selected at random with replacement from its respective bootstrap sample. That is, $\kappa$ for Jan 1st in year 1 of the projection is sampled from the Jan 1st bootstrap sample, and so on throughout year 1, repeating the same for year 2, and so on. Then, cleans-in-place are scheduled and the individual cleaning effects are bootstrapped from the samples of estimated cleaning effects for each method of cleaning (Fig. 4). Then, element swaps and replacements are scheduled. Their effects are known and deterministic. Then the wear model is run to obtain the projected states of each element and the implied NPD for the train for each day of the projection, using the estimates of the other parameters for that train and the user-defined system recovery *R,* which in turn implies $\omega_i$. This is repeated 100 times to obtain the ensemble forecast (grey ribbon) and the ensemble mean (red pen).

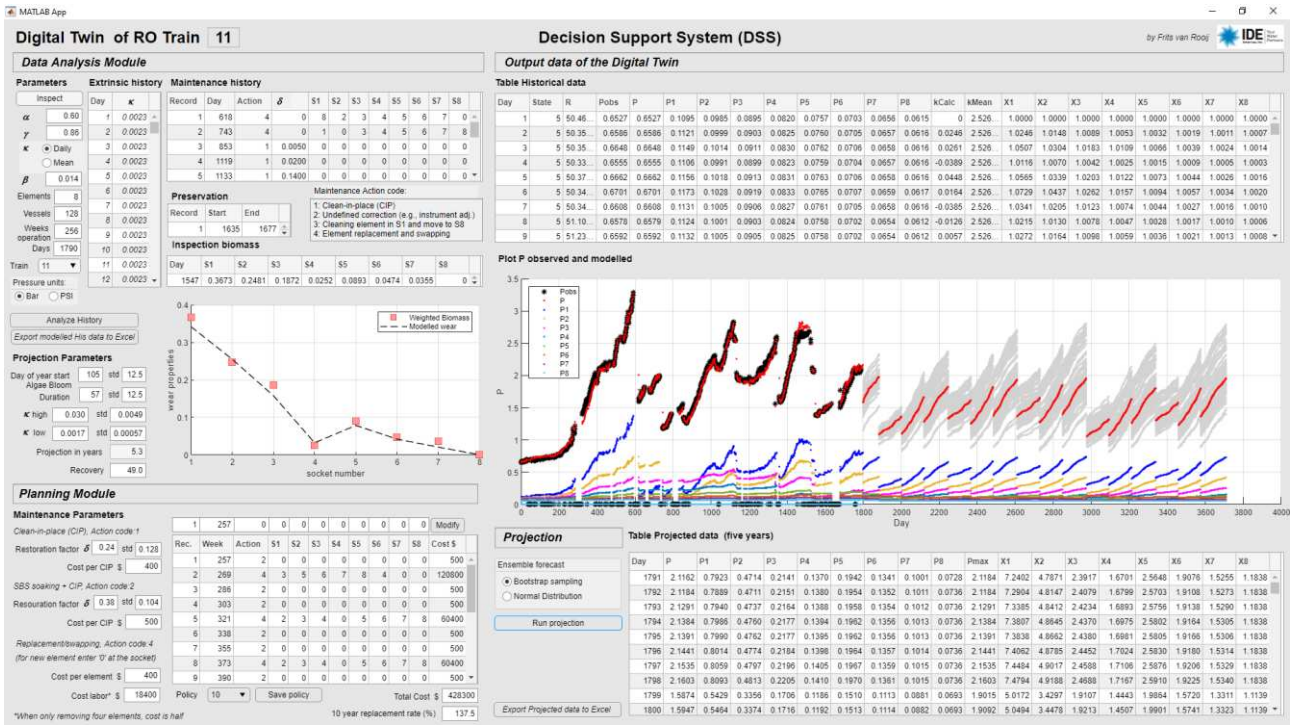


**Fig. 5.** Visualization of the decision support system (DSS). The plot at the left compares the weighted distribution of the biomass per element (red squares) against the modelled wear (black scatter line). The plot at the right shows the modelled trajectory of the NPD. The black markers represent the observed NPD, the red line, the modelled NPD.

## 6. Application to restoration policies

We compare 12 restoration policies over a planning horizon of five years, beginning in 2021 and ending in 2025, a point in time that will be ten years after the plant was commissioned. These policies use varying types and frequencies of cleaning, replacement, and swapping and are summarized in

Table 5. Membrane restoration can be undertaken without affecting the ability to deliver water according to the demand. Therefore, downtime is not included in the cost. Further, CIP is undertaken by the operators as part of their daily activities and does not involve additional labor cost. The cost in case of CIP is limited to chemicals consumed. In case of membrane replacement, both cost of elements and labor are considered.

**Table 5**

Policy description and comparison. Percentage replacement, numbers and types of cleans, and cost ($000s) for each year over the five-year planning horizon.

| | Policy 1 | | | | Policy 2 | | | | Policy 3 | | | |
|---|---|---|---|---|---|---|---|---|---|---|---|---|
| Week | new (%) | C1 | C2 | cost | new (%) | C1 | C2 | cost | new (%) | C1 | C2 | cost |
| 269-320 (Year 2021) | 19 | 0 | 14 | 1,275 | 0 | 0 | 42 | 21 | 0 | 42 | 0 | 17 |
| 321-372 (Year 2022) | 16 | 0 | 14 | 1,094 | 25 | 0 | 28 | 1,705 | 25 | 42 | 0 | 1,708 |
| 373-424 (Year 2023) | 16 | 0 | 14 | 1,094 | 12.5 | 0 | 28 | 860 | 12.5 | 42 | 0 | 862 |
| 425-476 (Year 2024) | 16 | 0 | 14 | 1,094 | 12.5 | 0 | 28 | 860 | 12.5 | 42 | 0 | 862 |
| 477-528 (Year 2025) | 16 | 0 | 14 | 1,094 | 12.5 | 0 | 28 | 860 | 12.5 | 42 | 0 | 862 |
| Total | 83 | 0 | 70 | 5,652 | 62.5 | 0 | 154 | 4,305 | 62.5 | 0 | 0 | 4,312 |
| Total over 10 years | 139 | 33 | 101 | | 118.75 | 33 | 185 | | 118.75 | 243 | 31 | |
| | Policy 4 | | | | Policy 5 | | | | Policy 6 | | | |
| Week | new (%) | C1 | C2 | cost | new (%) | C1 | C2 | cost | new (%) | C1 | C2 | cost |
| 269-320 (Year 2021) | 0 | 0 | 42 | 21 | 0 | 0 | 42 | 21 | 0 | 42 | 0 | 17 |
| 321-372 (Year 2022) | 12.5 | 0 | 14 | 981 | 12.5 | 0 | 28 | 988 | 12.5 | 42 | 0 | 991 |
| 373-424 (Year 2023) | 25 | 0 | 14 | 1,698 | 12.5 | 0 | 28 | 1,705 | 12.5 | 42 | 0 | 991 |
| 425-476 (Year 2024) | 12.5 | 0 | 14 | 981 | 12.5 | 0 | 28 | 988 | 12.5 | 42 | 0 | 991 |
| 477-528 (Year 2025) | 12.5 | 0 | 14 | 981 | 12.5 | 0 | 28 | 988 | 12.5 | 42 | 0 | 991 |
| Total | 62.5 | 0 | 98 | 4,663 | 50 | 0 | 154 | 4,691 | 50 | 210 | 0 | 3,982 |
| Total over 10 years | 118.75 | 33 | 129 | | 106.25 | 33 | 185 | | 106.25 | 243 | 31 | |

| | Policy 7 | | | | Policy 8 | | | | Policy 9 | | | |
|---|---|---|---|---|---|---|---|---|---|---|---|---|
| Week | new (%) | C1 | C2 | cost | new (%) | C1 | C2 | cost | new (%) | C1 | C2 | cost |
| 269-320 (Year 2021) | 0 | 42 | 0 | 17 | 0 | 0 | 42 | 21 | 12.5 | 0 | 28 | 988 |
| 321-372 (Year 2022) | 37.5 | 42 | 0 | 2,425 | 0 | 0 | 42 | 21 | 12.5 | 0 | 28 | 988 |
| 373-424 (Year 2023) | 0 | 56 | 0 | 22 | 0 | 0 | 42 | 21 | 12.5 | 0 | 28 | 988 |
| 425-476 (Year 2024) | 0 | 56 | 0 | 22 | 0 | 0 | 42 | 21 | 12.5 | 0 | 28 | 988 |
| 477-528 (Year 2025) | 12.5 | 42 | 0 | 991 | 0 | 0 | 42 | 21 | 12.5 | 0 | 28 | 988 |
| Total | 50 | 210 | 0 | 3,478 | 0 | 0 | 210 | 105 | 62.5 | 0 | 140 | 4,942 |
| Total over 10 years | 106.25 | 243 | 31 | | 56.25 | 33 | 241 | | 118.75 | 33 | 171 | |

| | Policy 10 | | | | Policy 11 | | | | Policy 12 | | | |
|---|---|---|---|---|---|---|---|---|---|---|---|---|
| Week | new (%) | C1 | C2 | cost | new (%) | C1 | C2 | cost | new (%) | C1 | C2 | cost |
| 269-320 (Year 2021) | 19 | 0 | 28 | 1,275 | 0 | 28 | 14 | 18 | 12.5 | 0 | 28 | 988 |
| 321-372 (Year 2022) | 16 | 0 | 28 | 1,094 | 12.5 | 0 | 42 | 995 | 12.5 | 0 | 42 | 995 |
| 373-424 (Year 2023) | 16 | 0 | 28 | 1,094 | 12.5 | 0 | 42 | 995 | 12.5 | 0 | 42 | 995 |
| 425-476 (Year 2024) | 16 | 0 | 28 | 1,094 | 12.5 | 0 | 42 | 995 | 12.5 | 0 | 42 | 995 |
| 477-528 (Year 2025) | 16 | 0 | 28 | 1,094 | 12.5 | 0 | 42 | 995 | 12.5 | 0 | 42 | 995 |
| Total | 83 | 0 | 140 | 5,652 | 50 | 28 | 182 | 4,000 | 62.5 | 0 | 196 | 4,970 |
| Total over 10 years | 139.25 | 33 | 101 | | 106.25 | 61 | 213 | | 118.75 | 33 | 227 | |

We start by describing the status quo (Policy 1). Element replacements to date were either one or two elements per vessel at each intervention. Replacement is replicated in all vessels of a train. Having experienced annual algal blooms for five years in a row, the O&M team assumed that over the five-year planning horizon 16% of the elements must be replaced annually (one element per vessel per year for 4 of 5 years and two elements per vessel in the other year). Further, due to COVID-related restrictions, replacement in 2020 diverged from the plan and replacement was two elements/vessel for only one train and one element/vessel for the other trains. In 2021, the plan is to

catch up from the previous year. Replacement for 2021 will be two elements/vessel for seven trains and one element/vessel for the others. This will bring the total element-replacement rate to 139% over ten years.

The current O&M procedure, when replacing one element per vessel at an intervention, discards the element in S1 and arranges the elements in the eight sockets as 234N5678. Thus, the element in S2 is placed in S1, that in S3 in S2, that in S4 in S3, a new element (N) is placed in S4, and the tail of the vessel (S5-S8) is unchanged. Locating the new element in socket 4, rather than socket 8, has the advantage that only the feed (seawater) side of the vessel needs to be opened and four elements removed. This is cheaper and quicker than opening the entire vessel. When replacement is two elements per vessel, the elements in S1 and S2 are discarded and the new and remaining elements are arranged as 356784NN.

Current cleaning policy is one C2 per train per year. O&M would like to do two C2 per train annually. Thus, Policy 10 is as Policy 1 but with two instances of C2 per train per year. Due to the commissioning of a new brine dilution system, all trains were offline for almost the whole period of the algae bloom in 2020. Therefore, Policies 2-7 have no replacement in 2021. Policies 2 and 3 have one instance of 356784NN in every train in 2022 and then one instance of 234N5678 in every train in every year thereafter. Their cleaning methods and frequencies differ. Every other policy, except policy 7, does 2356784N at the first replacement and then either 2345678N or 345678NN thereafter. This increases the time and labour, but all elements are replaced over time. Policy 7 does a three-element replacement (56784NNN). Policy 8 has only CIP (3 x C2 annually) to investigate if biofouling can be controlled by increasing CIP only. Policy 8, 11 and 12 require a minor upgrade of the CIP system so that the neutralization tank can be used for the discharge of used cleaning chemicals, shortening the preparation time for CIP significantly. Currently, the time duration of the discharge is a bottleneck that limits the frequency of C2 to two per train annually. Policies 11 and 12 suppose that the system is upgraded in 2021.

A policy is deemed admissible if the projected NPD is always below the critical threshold of 3.5 bar. We define risk as the proportion of daily NDP values in the projection that are above this threshold. This provides a measure of the likelihood that the PD goes critical. Above the 3.5 bar, elements can fail irrecoverably. Since there is a slight variance between the NPD and the underlying PD, we simultaneously consider two risk thresholds at 3 and 3.5 bar (Fig. 6). For a policy, the DSS calculates the proportion of the maximum (over the ensemble) projected daily NPD values above these thresholds for each train. This is the risk measure in Fig. 7.

From Fig. 7 we conclude that only Policies 10-12 have an acceptable risk (median < 15% on the conservative risk measure), and Policy 12 stands out in terms of risk and cost. Although the risk measure decreases with the strength of smoothing, we see no change in the risk ranking of the policies. At the same time, a longer smoothing window for the estimated feed quality provides clearer differentiation between algae bloom and non-algae bloom periods. As our purpose is to demonstrate the DSS, we do not discuss competing policies further. Instead, we note: a) policy choice is a multi-criteria one [48]; b) different policies might be used for different trains.

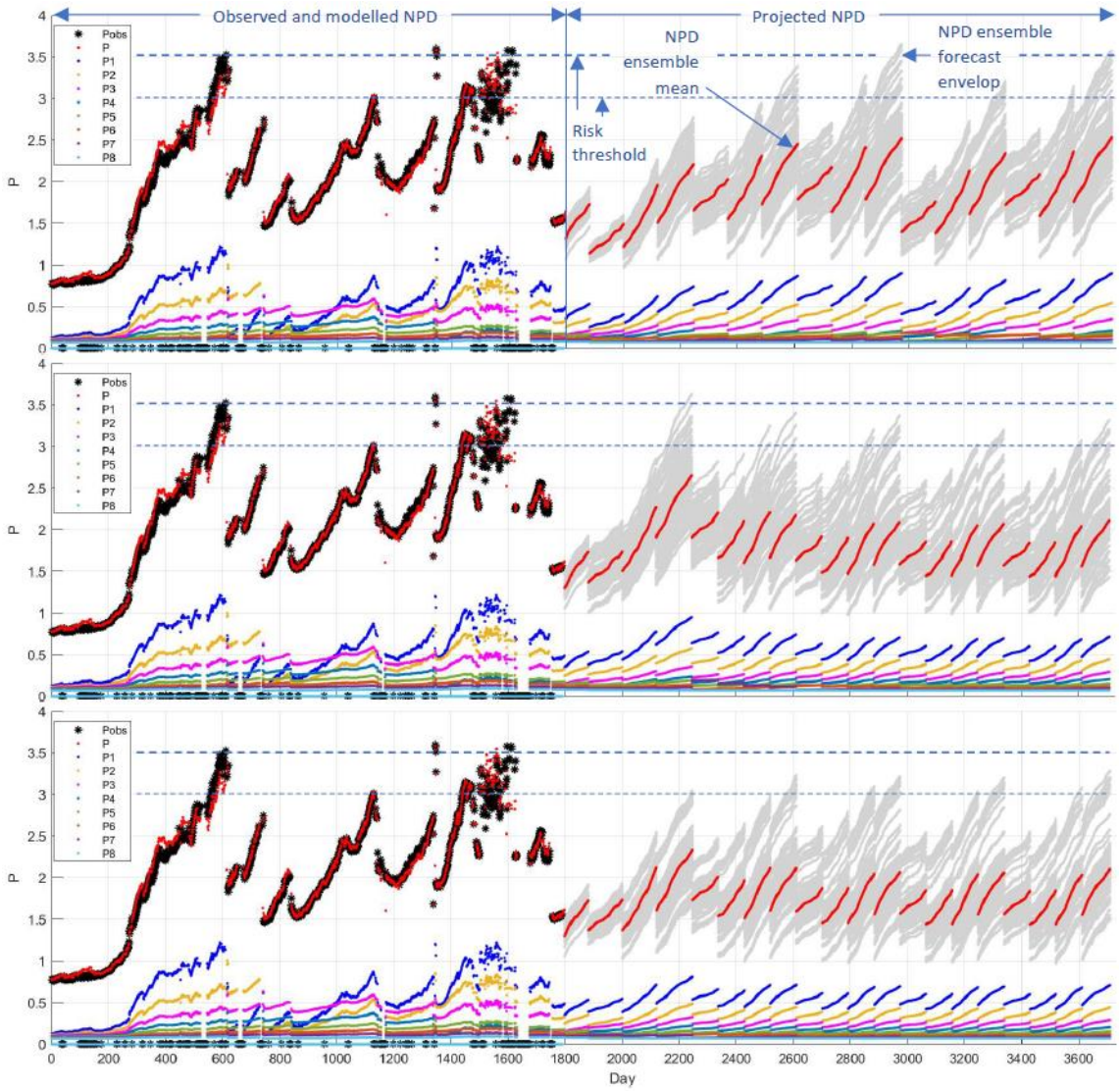


**Fig. 6.** NPD projection for train 1 for policies 10 (top), 11 (middle) and 12 (bottom). The risk measure is the proportion of days the grey ribbon is above the 3 or 3.5 bar threshold.

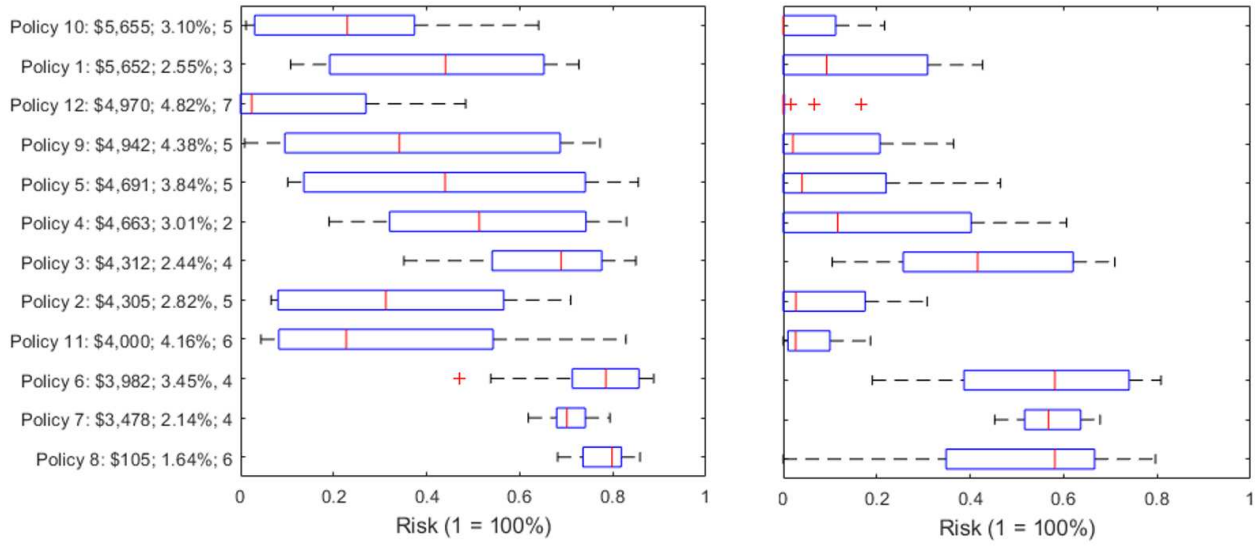


**Fig. 7.** Risk analysis of the policies with (-4,16) smoothing. Policies ranked by total cost ($000s) over five years and showing downtime per train (%), number of stops per train per year, and boxplots of risk measure (left, 3 bar; right, 3.5 bar) across 14 trains.

## 7. Discussion and conclusion

We demonstrate a decision support system (DSS) for planning the restoration of membrane elements in a reverse-osmosis (RO) desalination plant. The basis of the DSS is a mathematical model of wear and repair of the membrane elements. The wear of the elements is driven by biofouling due to annual algal blooms. The mathematical model is implemented as a simulation application, a digital twin (DT) of an RO train. The purpose of the DSS is to allow the operations and maintenance (O&M) company to prepare good long-term cost projections for different, competing restoration plans.

Approaches in the literature to date generally describe a membrane system and its associated wear as a single system. In our approach, the DT reveals the hidden states of individual elements in a vessel. This allows the study of the deterioration of a unique multi-component system in which components (elements) can be swapped and/or individually replaced. This is achieved by modeling wear at an individual element level.

We estimate the parameters of the model for each train using measurements of the differential pressure, which is continuously monitored. We parameterize the biofouling-position effect (lead elements tend to wear at a faster rate than trailing elements) and use the deviation of the measured distribution of biomass from the modelled wear to estimate the parameter. Other parameters are estimated using particle filtering. Our results show a good fit between the observed and the modelled states of the trains.

In particular, competing policies can be compared on the basis of risk, cost, downtime, and number of stoppages. Projections indicate that significant cost-saving can be achieved while not compromising the integrity of the train, the element-replacement rate can be reduced by 50 to 80%, and potential cost-reduction can outweigh the cost to upgrade the clean-in-place system. In general, the DSS has the potential for implementation at other plants, and in our opinion, it could become the gold-standard for membrane restoration management in the industry.

This study has focused on wear due to biofouling. For brackish water RO systems, a combination of biofouling and mineral scaling can occur, so that wear of leading elements combines with wear of trailing elements due to different circumstances. A modification of our mathematical model can accommodate these different wear factors. The DSS would remain the same in principle.

The DT has a number of limitations because necessarily the model is a simplification of the reality. Wear is modelled deterministically and so the DT may underestimate projected variation in PD. The model does not take into account other factors of long-term wear, for example, decreasing salt rejection due to ageing of elements. The DT uses a fixed recovery for the projection, whereas the recovery varies seasonally and with demand. We will address these in future development of the work. Also, over time, more information will be available from weighing and testing individual elements, and estimates of parameters can be updated. Finally, validating the model at other seawater RO plants around the world will be valuable, while noting that the Carlsbad plant uses only one element-type for its 1$^{st}$ pass RO vessels, so that plant with a hybrid configuration, that is, a combination of different element types in a vessel, will require some modification of the DT.

**References**


[1] C. Gaskin-Reyes, Water Planet: The Culture, Politics, Economics, and Sustainability of Water on Earth: The Culture, Politics, Economics, and Sustainability of Water on Earth., Santa Barbara, California: ABC-CLIO, 2016.

[2] R. Bashitialshaaer, "Solar-Energy Innovative and Sustainable Solution for Freshwater and Food Production for Lake Titicaca Islands," *EJERS, European Journal of Engineering Research and Science,* vol. 5, no. 4, pp. 436-442, 2020.

[3] G. G. Haile, Q. Tang, W. Li, X. Liu and X. Zhang, "Drought: Progress in broadening its understanding," *Wiley Interdisciplinary Reviews: Water,* vol. 7, no. 2, 2020.

[4] S. Jiang, Y. Li and B. P. Ladewig, "A review of reverse osmosis membrane fouling and control strategies," *Science of the Total Environment,* vol. 595, p. 567–583, 2017.

[5] S. Kerdi, A. Qamar, A. Alla Alpatova, J. S. Vrouwenvelder and N. Ghaffour, "Membrane filtration performance enhancement and biofouling mitigation using symmetric spacers with helical filaments," *Desalination,* vol. 484, 2020.

[6] M. Jafari, M. Vanoppen, J. van Agtmaal, E. Cornelissen, J. Vrouwenvelder, A. Verliefde, M. van Loosdrecht and C. Picioreanu, "Cost of fouling in full-scale reverse osmosis and nanofiltration installations in the Netherlands," *Desalination,* vol. 500, 2021.

[7] Y.-T. Chiou, M.-L. Hsieh and H.-H. Yeh, "Effect of algal extracellular polymer substances on UF membrane fouling," *Desalination,* vol. 250, p. 648–652, 2010.

[8] L. O. Villacorte, Y. Ekowati, H.Winters, G. Amya, J. Schippers and M. Kennedya, "MF/UF rejection and fouling potential of algal organic matter from bloom-forming marine and freshwater algae," *Desalination,* vol. 367, p. 1–10, 2015b.

[9] S. Li, H. Winters, L. Villacorte, Y. Ekowati, A.-H. Emwas, M. Kennedy and G. Amy, "Compositional similarities and differences between transparent exopolymer particles (TEPs) from two marine bacteria and two marine algae: Significance to surface biofouling," *Marine Chemistry,* vol. 174, p. 131–140, 2015.

[10] L. O. Villacorte, Y. Ekowati, H. Calix-Ponce, V. Kisielius, J. Kleijn, J. Vrouwenvelder, J. Schippers and M. Kennedy, "Biofouling in capillary and spiral wound membranes facilitated by marine algal bloom," *Desalination,* vol. 424, p. 74–84, 2017.

[11] L. O. Villacorte, S. A. A. Tabatabai, D. M. Anderson, G. L. Amy, J. C. Schippers and M. D. Kennedy, "Seawater reverse osmosis desalination and (harmful) algal blooms," *Desalination,* vol. 360, p. 61–80, 2015a.

[12] A. Matin, Z. Khan, S. Zaidi and M. Boyce, "Biofouling in reverse osmosis membranes for seawater desalination: Phenomena and prevention," *Desalination,* vol. 281, p. 1–16, 2011.

[13] M. Badruzzaman, N. Voutchkov, L. Weinrich and J. G. Jacangelo, "Selection of pretreatment technologies for seawater reverse osmosis plants: A review," *Desalination,* vol. 449, pp. 78-91, 2019.

[14] E. Koutsakos and D. Moxey, "Membrane Management System," *Desalination,* vol. 203, p. 307–311, 2007.

[15] A. Matin, T. Laoui, W. Falath and M. Farooque, "Fouling control in reverse osmosis for water desalination & reuse: Current practices & emerging environment-friendly technologies," *Science of the Total Environment,* pp. 1-20, 2020.

[16] S. S. Mitra, M. K. Sharma, S. Rybar, C. Bartels and L. Pelegrin, "Fujairah SWRO — management of membrane replacement," *Desalination and Water Treatment,* vol. 10, no. 1-3, pp. 255-264, 2009.

[17] J. Vrouwenvelder, S. Bakker, L. Wessels and J. van Paassen, "The Membrane Fouling Simulator as a new tool for biofouling control of spiral-wound membranes," *Desalination,* vol. 204, p. 170–174, 2007.

[18] A. R. Bartman, E. Lyster, R. Rallo, P. D. Christofides and Y. Cohen, "Mineral scale monitoring for reverse osmosis desalination via real-time membrane surface image analysis," *Desalination,* vol. 273, p. 64–71, 2011.

[19] L. Bian and N. Gebraeel, "Stochastic framework for partially degradation systems with continuous component degradation-rate-interactions.," *Naval Research Logistics,* vol. 61, pp. 286-303, 2014.

[20] R. Assaf, P. Do, S. Nefti-Meziani and P. Scarf, "Wear rate–state interactions within a multi-component system: a study of a gearbox-accelerated life testing platform," *Journal of Risk and Reliability,* vol. 232, no. 4, p. 425–434, 2018.

[21] L. A. Bereschenko, A. J. M. Stams, J. W. Euverink and M. C. M. van Loosdrecht, "Biofilm Formation on Reverse Osmosis Membranes Is Initiated and Dominated by Sphingomonas spp.," *Applied and Environmental Microbiology,* vol. 76, no. 8, p. 2623–2632, 2010.

[22] T. D. Wolfe, "Membrane Process Optimization Technology," United States Department of the Interior Bureau of Reclamation, Grass Valley, California, 2003.

[23] T. Zhou, E. L. Droguett and M. Modarres, "A common cause failure model for components under age-related degradation," *Reliability Engineering and System Safety,* vol. 195, 2020.

[24] M. Zamanillo, E. Ortega-Retuerta, S. Nunes, P. Rodríguez-Ros, M. Dall'Osto, M. Estrada, M. Montserrat Sala and R. Simó, "Main drivers of transparent exopolymer particle distribution across the surface Atlantic Ocean," *Biogeosciences,* vol. 16, p. 733–749, 2019.

[25] P. Stoodley, K. Sauer, D. Davies and J. Costerton, "Biofilm as Complex Differentiated Communities," *Annual Review of Microbiology,* vol. 56, no. 1, pp. 187-209, 2002.

[26] R. Nicolai and R. Dekker, "Optimal Maintenance of Multi-component Systems: A Review," in *Complex System Maintenance Handbook*, K. A. H. Kobbacy and D. N. P. Murthy, Eds., London, Springer Series in Reliability Engineering, 2008, pp. 263-286.

[27] B. Iung, P. Do, E. Levrat and A. Voisin, "Opportunistic maintenance based on multi-dependent components of manufacturing system," *CIRP Annals - Manufacturing Technology,* vol. 65, p. 401–404, 2016.

[28] P. Do, R. Assaf, P. Scarf and B. Iung, "Modelling and application of condition-based maintenance for a two-component system with stochastic and economic dependencies.," *Reliability Engineering & System Safety,* vol. 182, pp. 86-97, 2019.

[29] B. de Jonge and P. A. Scarf, "A review on maintenance optimization," *European Journal of Operational Research,* pp. 805-824, 2020.

[30] Y. Fu, T. Yuan and X. Zhu, "Optimum Periodic Component Reallocation and System Replacement Maintenance," *IEEE Transactions on Reliability,* vol. 68, pp. 753-763, 2019.

[31] A. Najem and F. Coolen, "Cost effective component swapping to increase system reliability," Manchester, UK, 2018.

[32] J. u. Geng, M. Azarian and M. Pecht, "Opportunistic maintenance for multi-component systems considering structural dependence and economic dependence," *Journal of Systems Engineering and Electronics,* vol. 26, no. 3, pp. 493 - 501, 2015.

[33] C. D. Dao and M. J. Zuo, "Selective maintenance of multi-state systems with structural dependence," *Reliability Engineering and System Safety,* vol. 159, pp. 184-195, 2017.

[34] M. C. A. Olde Keizer, S. D. P. Flapper and R. H. Teunter, "Condition-based maintenance policies for systems with multiple dependent components: A review," *European Journal of Operational Research,* vol. 261, pp. 405-420, 2017.

[35] P. A. Scarf and M. Deara, "Block Replacement Policies for a Two-Component System with Failure Dependence," *Naval Research Logistics,* vol. 50, pp. 70-87, 2003.

[36] H. Ascher and H. Feingold, Repairable systems reliability : modeling, inference, misconceptions and their causes, New York: Marcel Dekker, 1984.

[37] D. Brkić, "Discussion of‘Jacobian Matrix for SolvingWater Distribution System Equations withthe Darcy-Weisbach Head-Loss Model” byAngus Simpson and Sylvan Elhay," *Journal of hydraulic engineering,* vol. 128, no. 11, pp. 1000-1001, 2012.

[38] T. J. Battin, L. A. Kaplan, J. D. Newbold and C. M. E. Hansen, "Contributions of microbial biofilms to ecosystem processes in stream mesocosms," *Nature,* vol. 426, pp. 439-441, 2003.

[39] N. Kantas, A. Doucet, S. S. Singh, J. Maciejowski and N. Chopin, "On Particle Methods for Parameter Estimation in State-Space Models," *Statistical Science,* vol. 30, no. 3, pp. 328-351, 2015.

[40] A. Doucet, N. d. Freitas and N. Gordon, "An Introduction to Sequential Monte Carlo Methods," in *Sequential Monte Carlo Methods in Practice. Statistics for Engineering and Information Science*, A. Doucet, N. d. Freitas and N. Gordon, Eds., New York, NY, Springer, 2001, pp. 3-14.

[41] Do, F. Van Rooij, P.A. Scarf (2021) Modelling wear and repair of a multi-component system with structural, economic and stochastic dependencies: the case of membranes in reverse-osmosis desalination. *Working paper.*

[42] R. W. Schafer, "What Is a Savitzky-Golay Filter?," *IEEE Signal processing magazine,* pp. 111-117, 2011.

[43] M. R. Chernick and R. A. LaBudde, An Introduction to Bootstrap Methods with Applications to R, New Jersey: Wiley, 2011.

[44] E. J. Tuegel, A. R. Ingraffea, T. G. Eason and S. M. Spottswood, "Reengineering Aircraft Structural Life Prediction Using a Digital Twin," *International Journal of Aerospace Engineering,* vol. 2011, 2011.

[45] W. Kritzinger, M. Karner, G. Traar, J. Henjes and W. Sihn, "Digital Twin in manufacturing: A categorical literature review and classification," in *IFAC (International Federation of Automatic Control)*, Seville, Spain, 2018.

[46] S. Haag and R. Anderl, "Digital twin – Proof of concept," *Manufacturing Letters,* vol. 15, p. 64–66, 2018.

[47] E. Elsayed, "Accelerated Life Testing," in *Handbook of Reliability Engineering*, London, Springer, 2003, pp. 415-428.

[48] A. T. de Almeida, R. J. P. Ferreira and C. A. V. Cavalcante, "A review of the use of multicriteria and multi-objective models in maintenance and reliability," *IMA Journal of Management Mathematics,* vol. 26, no. 3, p. 249–271, 2015